Jurnal Rekayasa Mesin
p-ISSN: 1411-6863, e-ISSN: 2540-7678
Vol.21, No.1, April **2026**, hal. 67-74

Optimisation of Preheating Temperature for Mechanical Performance of SMAW Welded ASTM A36 Steel

Sumarji[1*], Agus Hariyanto[2], Wajilan[2], FX. Arif Wahyudianto[3], Agus Suprihanto[1]
[1]Department of Mechanical Engineering Fakultas Teknik, Program Studi Magister Teknik Mesin, Universitas Diponegoro
Jl. Prof. Sudarto, S.H. Tambalang Semarang
[2]Department of Mechanical Engineering, Politeknik Negeri Samarinda-Samarinda-Indonesia
Jl. Cipto Mangunkusumo, Kampus Gunung Lipan, Sungai Keledang, Kota Samarinda, Kalimantan Timur, Indonesia
[3]Department of Mechanical Engineering, Semarang State Polytechnic, Semarang, 50275, Indonesia
Jl. Prof. Soedarto, Tembalang, Kota Semarang, Jawa Tengah
*E-mail: marjismr@gmail.com

Submitted: 06-01-2026; Accepted: 25-04-2026; Published: 30-04-2026

Abstract

The Shielded Metal Arc Welding (SMAW) process applied to ASTM A36 structural steel generates thermal cycles that influence the mechanical behaviour of welded joints. This study investigates the effect of preheating temperature on tensile properties and hardness distribution of SMAW-welded ASTM A36 steel plates with a thickness of 10 mm. Preheating temperatures of none, 150 °C, 250 °C, and 350 °C were applied prior to welding in the 1G position using AWS A5.1 E7016 and E7018 electrodes. Tensile testing was conducted according to ASTM E8, while Vickers hardness measurements were performed across the base metal (BM), heat-affected zone (HAZ), and weld metal (WM). The results show a consistent hardness distribution of WM > HAZ > BM for all preheating conditions, with average hardness values ranging from 190–210 HV in the WM, 179–186 HV in the HAZ, and 164–173 HV in the BM. The yield strength increased from 301.69 MPa (without preheating) to 315.68 MPa at 250 °C, followed by a decrease to 298.70 MPa at 350 °C, which is associated with microstructural softening. In contrast, the ultimate tensile strength remained relatively stable within the range of 443–446 MPa. Based on these results, preheating at 250 °C tends to provide a more homogeneous hardness distribution and higher yield strength, suggesting a more favourable thermal condition for improving the mechanical performance of SMAW-welded ASTM A36 steel.

Keywords: Preheating; SMAW; ASTM A36 steel; Tensile strength; Vickers hardness

Abstrak

Proses pengelasan *Shielded Metal Arc Welding* (SMAW) yang diterapkan pada baja struktural ASTM A36 menghasilkan siklus termal yang mempengaruhi perilaku mekanik sambungan las. Penelitian ini mengkaji pengaruh temperatur *preheating* terhadap sifat tarik dan distribusi kekerasan pada pelat baja ASTM A36 hasil pengelasan SMAW dengan ketebalan 10 mm. Variasi temperatur *preheating* yang digunakan meliputi tanpa pemanasan awal, 150 °C, 250 °C, dan 350 °C, yang diterapkan sebelum proses pengelasan pada posisi 1G menggunakan elektroda AWS A5.1 E7016 dan E7018. Pengujian tarik dilakukan sesuai standar ASTM E8, sedangkan pengujian kekerasan Vickers dilakukan pada daerah *base metal* (BM), *heat-affected zone* (HAZ), dan *weld metal* (WM). Hasil penelitian menunjukkan bahwa distribusi kekerasan mengikuti pola konsisten WM > HAZ > BM pada seluruh kondisi *preheating*, dengan nilai kekerasan rata-rata berkisar antara 190–210 HV pada WM, 179–186 HV pada HAZ, dan 164–173 HV pada BM. Nilai *yield strength* meningkat dari 301,69 MPa pada kondisi tanpa *preheating* menjadi 315,68 MPa pada temperatur 250 °C, kemudian menurun menjadi 298,70 MPa pada temperatur 350 °C yang berkaitan dengan pelunakan mikrostruktur. Sebaliknya, nilai *ultimate tensile strength* relatif stabil pada kisaran 443–446 MPa. Berdasarkan hasil tersebut, *preheating* pada temperatur 250 °C cenderung menghasilkan distribusi kekerasan yang lebih homogen serta nilai *yield strength* yang lebih tinggi, yang menunjukkan kondisi termal yang lebih baik dalam meningkatkan kinerja mekanik sambungan las SMAW pada baja ASTM A36.

Kata kunci: Preheating; SMAW; ASTM A36; Kekuatan tarik; Kekerasan Vickers

1. Introduction

The *Shielded Metal Arc Welding* (*SMAW*) process is extensively utilised in structural steel fabrication due to its operational adaptability and economic feasibility. Nevertheless, the thermal cycles generated during welding introduce steep temperature gradients, which significantly influence microstructural evolution and mechanical performance in

low-carbon steels such as ASTM A36. These effects are primarily governed by variations in heat input and cooling rate [1,2]. In such materials, thermal fluctuations may lead to non-uniform hardness distribution within the *heat-affected zone* (*HAZ*), thereby potentially reducing the structural reliability of welded joints [3].

It is well recognised that welding thermal conditions, particularly heat input and cooling rate, play a crucial role in controlling phase transformation behaviour in carbon steels [4,5]. Variations in cooling rate during welding dictate the formation of ferrite–pearlite microstructures, where slower cooling tends to produce coarser ferrite grains with lower hardness, while faster cooling promotes finer microstructures accompanied by higher hardness gradients [6]. Furthermore, insufficient thermal control can increase susceptibility to *hydrogen-induced cracking*, especially in the *HAZ*, due to the combined influence of diffusible hydrogen, residual stresses, and microstructural heterogeneity [7].

Preheating is commonly employed as an effective thermal management strategy to mitigate temperature gradients, reduce cooling rates, and limit the development of residual stresses [8,9]. Previous studies have demonstrated that preheating contributes to improved hardness distribution and stabilisation of tensile properties in welded joints [10]. Specifically, in ASTM A36 steel welded using the *SMAW* process, preheating has been shown to affect both hardness evolution and tensile behaviour through modification of the welding thermal cycle [11,12].

Despite these observations, most existing studies tend to describe general trends without establishing a clear mechanistic relationship between preheating temperature, hardness distribution, and yield strength in *SMAW* welds of ASTM A36 steel. In particular, the metallurgical justification for selecting an intermediate preheating temperature, such as 250 °C, remains inadequately explained in relation to ferrite–pearlite transformation mechanisms and cooling rate control. This gap introduces uncertainty in determining optimal welding conditions that ensure a balanced combination of strength, ductility, and microstructural stability.

Accordingly, this study aims to evaluate the effect of preheating temperature variations (N/A, 150 °C, 250 °C, and 350 °C) on tensile strength and hardness distribution in *SMAW*-welded ASTM A36 steel. The novelty of this research lies in establishing an experimentally supported correlation between preheating temperature, hardness gradient, and yield strength under controlled welding parameters. It is hypothesised that moderate preheating (approximately 250 °C) can effectively reduce thermal gradients and cooling rates, resulting in a more homogeneous ferrite–pearlite microstructure, enhanced yield strength, and a more uniform hardness profile without inducing excessive thermal softening.

2. Material and Method

2.1. Materials and Specimen Preparation

The material used was ASTM A36 low-carbon steel plate with a thickness of 10 mm. The plates were cut into 150 mm × 300 mm specimens and prepared with a single V-groove joint (60° groove angle, 2 mm root face, and 2 mm root gap).

2.2. Welding Procedure

Welding was performed using the Shielded Metal Arc Welding (SMAW) process in the flat position (1G). AWS A5.1 E7016 (Ø 2.6 mm) electrodes were used for the root pass, while AWS A5.1 E7018 (Ø 3.2 mm, LB-52) electrodes were used for filler and capping passes.

The welding parameters were maintained constant, with a current of 90–110 A (root) and 110–130 A (filler/capping), voltage of 20–25 V, and travel speed of 2–3 mm/s. Welding was carried out using a three-pass technique (root, filler, and capping), with interpass temperature controlled below 150 °C.

The heat input was calculated as:

$$\textit{Heat Input}\ (\mathrm{HI}) = \frac{\mathrm{V \times I \times 60}}{\mathrm{S \times 1000}} \times 0{,}8$$

where H is heat input (kJ/mm), V is voltage (V), I is current (A), S is welding speed (mm/min), and $Efficienc$ 0,8

2.3. Preheating Procedure

Preheating was applied at N/A, 150 °C, 250 °C, and 350 °C using an electric heater. Temperature was monitored using a K-type thermocouple and maintained within ±10 °C of the target. Specimens were held for approximately 10 minutes prior to welding to ensure uniform heating.

2.4. Cooling Conditions

All specimens were cooled under ambient air conditions without forced cooling. The cooling rate was governed by natural convection.

2.5. Mechanical Testing

2.5.1. Hardness Test

Vickers hardness testing was performed according to ASTM E92 using a load of 300 gf and a dwell time of 15 s. Measurements were taken across BM, HAZ, and WM regions with a spacing of 0.5 mm.

2.5.2. Tensile Test

Tensile testing was conducted according to ASTM E8/E8M. The weld joint was positioned at the center of the specimen. Three specimens were tested for each condition, and results were reported as mean values with standard deviation.

2.6. Microstructural Analysis

Microstructural observations were conducted using optical microscopy (OM). Specimens were prepared by grinding, polishing, and etching with 2% Nital. The analysis focused on ferrite–pearlite phases and grain morphology in BM, HAZ, and WM regions.

2.7. Statistical Analysis

Experimental data were analysed using mean values and standard deviation to evaluate data consistency.

2.8. Specimen Geometry

The tensile specimen geometry and weld position are illustrated in Fig. 1, with the weld located at the center of the gauge length.

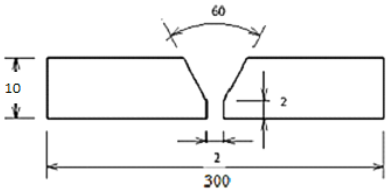

Figure 1. V-groove weld joint geometry

3. Results and Discussion

3.1 Chemical Composition Test

Tabel 1. Chemical composition of ASTM A36 steel

Element	Measured (%)	ASTM A36 (max %)
C	0.21	≤ 0.25–0.29
Mn	0.85	≤ 1.20
P	0.018	≤ 0.040
S	0.012	≤ 0.050

The chemical composition of ASTM A36 steel was analysed using optical emission spectroscopy (OES), and the results are presented in Table 1. The measured values of C, Mn, P, and S are within the allowable limits of ASTM A36

standard, indicating that the material is representative of typical low-carbon structural steel. Therefore, the mechanical behaviour observed in this study is primarily influenced by welding parameters rather than compositional variations.

3.2. Vickers Hardness Testing

From the vickers hardness test that has been carried out, hardness data from each area of WM, HAZ, and BM can be seen in Table 2.

Tabel 2. Hardness Test Results Data

Temperature	WM	HAZ	BM	SD_WM	SD_HAZ	SD_BM
N/A	190,08	178,36	164,67	6,27	1,66	3,1
150 ^{0}C	199,54	184,68	171,32	7,36	1,13	3,42
250 ^{0}C	209,94	191,28	173,04	2,96	7,6	3,61
350 ^{0}C	198,46	182,87	166,19	9,09	4,49	4,8

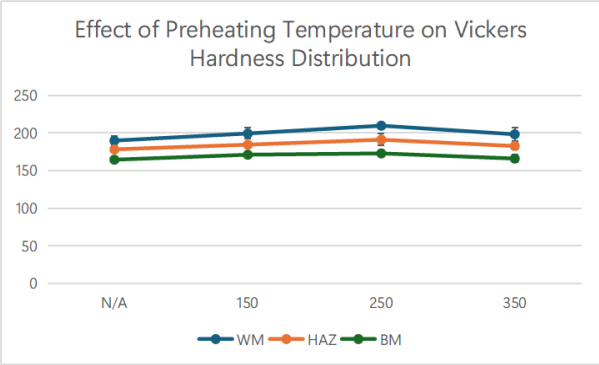

Figure 2. Effect of preheating temperature on Vickers hardness of WM, HAZ, and BM (mean ± SD)

The distribution of Vickers hardness consistently follows the trend *WM* > *HAZ* > *BM* under all preheating conditions, indicating the influence of varying thermal cycles and cooling rates during the welding process [13]. The hardness of the *base metal* (*BM*) ranges between 164–173 HV and shows an increasing tendency up to a preheating temperature of 250 °C, which reflects reduced thermal gradients and enhanced. The *heat-affected zone* (*HAZ*) exhibits higher hardness compared to the *BM*, with maximum values observed at 250 °C. This condition indicates a more controlled and uniform thermal cycle at intermediate preheating levels [14]. Meanwhile, the *weld metal* (*WM*) demonstrates the highest hardness values (190–210 HV), primarily governed by solidification characteristics and the chemical composition of the filler material.

In general, preheating at 250 °C results in a more uniform hardness distribution across the welded joint. This behaviour aligns with the fundamental role of preheating in moderating cooling rates and controlling phase transformation processes in low-carbon steel weldments.

3.3. Tensile Strength Testing

The tensile test results are presented in Table 3 and Fig 4. The post-fracture specimens for each preheating condition (N/A, 150 °C, 250 °C, and 350 °C) are shown in Fig 3. All specimens fractured in the base metal (BM) region, indicating that the weld joint strength is comparable to or higher than that of the base material. This suggests that the welding process produced sound joints without significant defects.

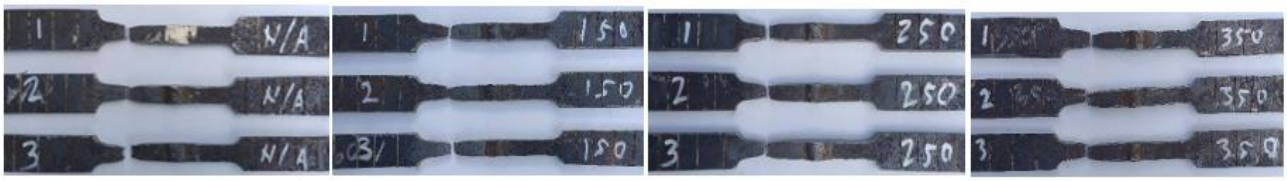

Figure 3. Fractured tensile specimens at different preheating temperatures

Table 3. Tensile Test Results Data

Temperature ^{0}C	UTS (MPa)	YS (MPa)	SD_UTS (MPa)	SD_YS (MPa)
N/A	446,13	301,68	3,82	5,06
150 ^{0}C	443,42	307,87	2,10	5,32
250 ^{0}C	444,87	315,68	1,03	11,05
350 ^{0}C	446,34	298,70	1,50	5,62

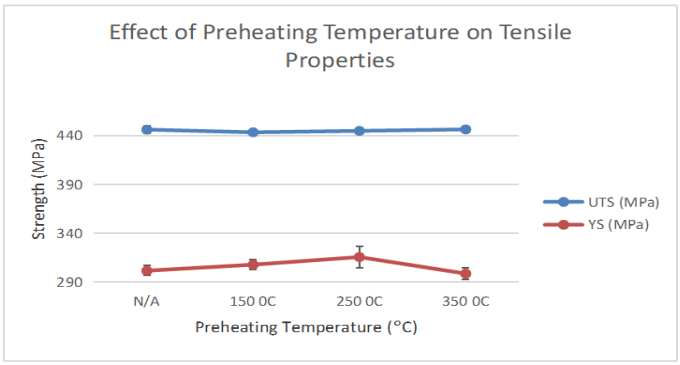

Figure 4. Tensile properties (UTS and YS) vs. preheating temperature (mean ± SD)

The results of tensile testing indicate that the *ultimate tensile strength* (*UTS*) varies within a relatively narrow range of 443–446 MPa, suggesting that preheating temperature has a limited effect on the ultimate strength of the welded joint. In contrast, the *yield strength* (*YS*) ranges from 298–316 MPa and demonstrates more pronounced variation, indicating greater sensitivity to thermal conditions during the welding process [15]. At *room temperature* (*RT*), the welded joint exhibits moderate *YS* despite relatively high *UTS*, implying a lower resistance to the onset of plastic deformation. The application of preheating at 150 °C leads to a slight increase in *YS*, while the highest value is obtained at 250 °C, reflecting enhanced resistance to deformation under intermediate thermal conditions. Conversely, at 350 °C, a reduction in *YS* is observed, which can be associated with thermal softening caused by excessive heat input [16]. Overall, preheating temperature exerts a more significant influence on *YS* than on *UTS*. Furthermore, the relatively higher standard deviation at 250 °C indicates greater variability in deformation behaviour. This trend is consistent with the role of preheating and heat input in governing microstructural evolution in welded ASTM A36 steel.

3.4. Microstructural Analysis

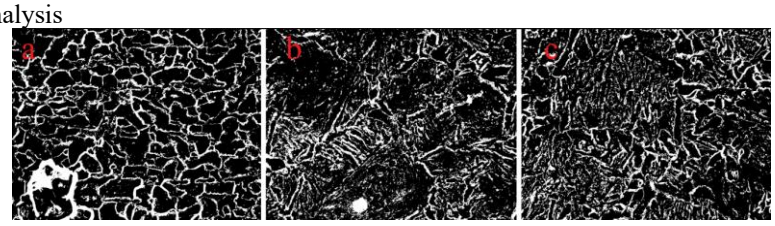

Figure 4. Microstructures of (a) BM, (b) HAZ, and (c) WM without preheating

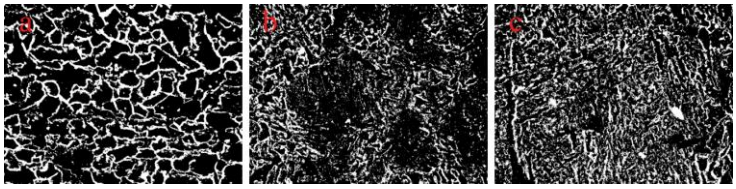

Figure 5. Microstructures of (a) BM, (b) HAZ, and (c) WM at 150°C preheating

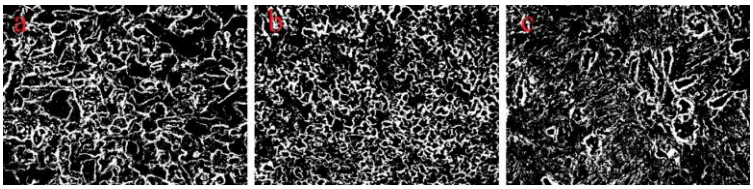

Figure 6. Microstructures of (a) BM, (b) HAZ, and (c) WM at 250°C preheating

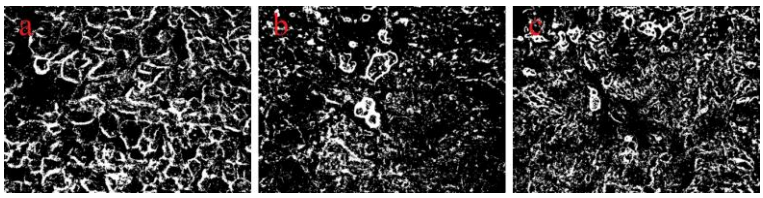

Figure 7. Microstructures of (a) BM, (b) HAZ, and (c) WM at 350°C preheating

Tabel 4. Ferrite–pearlite phase distribution and microstructural characteristics of SMAW welded A36 steel under different preheating conditions

Preheating Condition	Zone	Ferrite (%)	Pearlite (%)	Characteristics
N/A	BM	78–85	15–22	Stable base metal structure; minimally affected by welding heat
	HAZ	64–72	28–36	Transitional microstructure with localised grain coarsening due to steep thermal gradients
	WM	70–76	24–30	Refined solidification structure with a ferrite-dominant matrix and dispersed pearlite; relatively low thermal stability
150 °C	BM	77–84	16–23	Stable and homogeneous microstructure
	HAZ	66–73	27–34	Controlled grain growth; more homogeneous ferrite–pearlite distribution
	WM	72–78	22–28	Improved phase homogeneity; reduced thermal shock; moderate refinement
250 °C	BM	78–85	15–22	Stable base metal with negligible structural alteration
	HAZ	69–76	24–31	Improved microstructural stability; moderate grain growth
	WM	74–80	20–26	Most homogeneous solidification structure; balanced ferrite–pearlite distribution; optimal condition
350 °C	BM	77–84	16–23	Stable microstructure with slight grain coarsening
	HAZ	63–71	29–37	Pronounced grain growth; heterogeneous ferrite–pearlite distribution
	WM	70–76	24–30	Grain coarsening due to excessive thermal input; reduced refinement

The microstructural features summarised in Table 4 demonstrate that preheating temperature plays a decisive role in controlling phase distribution, microstructural evolution, and morphological stability across the *weld metal* (*WM*),

heat-affected zone (*HAZ*), and *base metal* (*BM*). This behaviour is consistent with the high thermal sensitivity of SMAW carbon steel weldments and the function of preheating in regulating transformation kinetics [17,18]. Under non-preheated conditions, steep thermal gradients tend to induce localised grain coarsening within the *HAZ*, whereas the *BM* maintains a relatively stable ferrite–pearlite structure due to limited thermal exposure, reflecting the influence of welding thermal cycles in low-carbon steels processed by SMAW [19].

Comparable observations have been reported in low-carbon steel welds, where preheating effectively reduces thermal gradients and enhances microstructural uniformity [9]. In the present study, a preheating temperature of 250 °C yields the most homogeneous ferrite–pearlite distribution, which can be attributed to a more balanced combination of heat input and cooling rate, influenced by the 10 mm plate thickness and the use of E7016/E7018 electrodes. Lower preheating at 150 °C is sufficient to partially mitigate thermal shock, whereas excessive preheating at 350 °C promotes increased atomic diffusion, resulting in grain coarsening and greater heterogeneity within the *HAZ* [20].

Accordingly, the observed microstructural evolution follows a refinement–stabilisation–coarsening progression, with 250 °C representing the most favourable condition for achieving an optimal balance between heat diffusion and cooling rate under the applied welding parameters.

4. Conclusion

This study demonstrates that preheating temperature strongly influences the mechanical performance and microstructural characteristics of SMAW-welded ASTM A36 steel. The hardness distribution consistently follows the pattern of WM > HAZ > BM, while yield strength (YS) shows greater sensitivity to preheating than ultimate tensile strength (UTS), with the highest YS observed at 250 °C. This condition is associated with a more homogeneous ferrite–pearlite distribution and improved hardness stability, indicating enhanced deformation resistance under intermediate thermal conditions.

However, this finding should be interpreted within the limitations of this study, as microstructural analysis was limited to optical observation without quantitative grain size measurement or advanced characterization techniques such as SEM or EBSD. In addition, the parameter range was restricted and statistical validation beyond standard deviation analysis was not performed. Future work is recommended to include detailed microstructural characterization, as well as investigations on residual stress, impact toughness, and fracture behaviour. Expanding the range of welding parameters and applying advanced statistical analysis would further improve the reliability of the findings for structural applications.

References

[1] A. Rifaldi, A. U. Ryadin, and A. R. Hakim, “Pengaruh Suhu Preheating Terhadap Kekuatan Tarik Dan Kekerasan Pelat Baja Astm a36 Pada Pengelasan Shielded Metal Arc Welding (Smaw),” *Sigma Tek.*, vol. 4, no. 1, pp. 81–90, 2021, doi: 10.33373/sigmateknika.v4i1.3216.

[2] B. H. Irawan, F. Dwi, P. Novian, and M. I. Saihilmi, “Experimental Study of the Effect of Preheating Process on Welded Joints of ASTM A36 Material on Mechanical Characteristics : Evaluation of Tensile , Bending , and Macrostructure,” vol. 25, no. 3, pp. 272–278, 2025.

[3] Y. Gu, X. W. Chen, H. H. Kang, C. G. Zhang, Z. X. Wang, and F. R. Xiao, “Effects of Chemical Composition on Welding HAZ Softening of High-Strength Pipeline Steels,” *Metals (Basel).*, vol. 15, no. 12, Dec. 2025, doi: 10.3390/met15121314.

[4] O. Falodun, S. Oke, and M. Bodunrin, *A comprehensive review of residual stresses in carbon steel welding : formation mechanisms , mitigation strategies , and advanced post - weld heat treatment techniques*, vol. 136, no. 10. Springer London, 2025. doi: 10.1007/s00170-025-15088-8.

[5] U. Metalografi, L. Korosi, S. Steel, A. Fazadima, H. Pratikno, and H. Ikhwani, "Analisis Pengaruh Variasi Heat Input terhadap Uji," vol. 11, no. 3, pp. 38–43, 2022.

[6] S. Senthilkumar, S. Manivannan, R. Venkatesh, and M. Karthikeyan, "Heliyon Influence of heat input on the mechanical characteristics , corrosion and microstructure of ASTM A36 steel welded by GTAW technique," *Heliyon*, vol. 9, no. 9, p. e19708, 2023, doi: 10.1016/j.heliyon.2023.e19708.

[7] L. Wang, H. Li, Y. Huang, K. Wang, and M. Zhou, "Effect of Preheating on Martensitic Transformation in the Laser Beam Welded AH36 Steel Joint : A Numerical Study," pp. 1–13, 2022, doi: 10.3390/met12010127.

[8] A. N. Idriss, A. Maleque, Z. Kamdi, and N. Muhammad, "The Preheating Effect of Mild Steel Layers Deposited using SMAW at 100 A and 70 A," vol. 1, no. 1, pp. 112–120, 2024.

[9] M. Thabrani, A. Hafizh, A. Rasyid, M. Arif, and T. Hartutuk, "Effect of Post-Welding Heat Treatment on ASTM A36 Steel on Tensile Strength," vol. 7, no. 2, pp. 36–42, 2025.

[10] A. Akbar, M. Mulyadi, and N. H. Wiyono, "Effect of preheating on the hardness and microstructure in Shielded Metal Arc Weldments of A283 B," *IOP Conf. Ser. Mater. Sci. Eng.*, vol. 1098, no. 6, p. 062113, 2021, doi: 10.1088/1757-899x/1098/6/062113.

[11] N. R. Oktaviandy, K. Kardiman, and R. Hanifi, "Effect of Preheat Temperature Variation with Cooling Media on Mechanical Properties in Welding SS400 Steel," *SINTEK J. J. Ilm. Tek. Mesin*, vol. 17, no. 2, p. 130, 2023, doi: 10.24853/sintek.17.2.130-142.

[12] M. Shafeek, S. Suranjan, D. Doreswamy, and H. K. Sachidananda, "Effect of welding parameters on microstructure and mechanical properties of GMAW welded S275 steel welded zone," *Discov. Mater.*, vol. 4, no. 1, Dec. 2024, doi: 10.1007/s43939-024-00169-4.

[13] K. Yang *et al.*, "Prediction of HAZ Microstructure and Hardness for Q960E Joints Welded by Triple-Wire GMAW Based on Thermal and Numerical Simulation," *Materials (Basel).*, vol. 14, no. 17, p. 4898, Aug. 2021, doi: 10.3390/ma14174898.

[14] C. Chen, G. Sun, W. Du, Y. Li, C. Fan, and H. Zhang, "Influence of heat input on the appearance, microstructure and microhardness of pulsed gas metal arc welded Al alloy weldment," *J. Mater. Res. Technol.*, vol. 21, pp. 121–130, Nov. 2022, doi: 10.1016/j.jmrt.2022.09.028.

[15] M. U. Pawara, A. Alamsyah, M. Syarif, F. Mahmuddin, and H. Harifuddin, "Effect of Post Weld Heat Treatment on Tensile Strength of ASTM A36 Welded Joints: Application on Hull Vessel Material," *Int. J. Mar. Eng. Innov. Res.*, vol. 8, no. 1, pp. 56–65, 2023, doi: 10.12962/j25481479.v8i1.16312.

[16] V. Kumar *et al.*, "An investigation of the effect of GMAW and SMAW processes on mechanical and microstructural properties of welded E350 grade steel," *Sci. Rep.*, vol. 15, no. 1, p. 36338, Oct. 2025, doi: 10.1038/s41598-025-20140-4.

[17] E. Surojo, R. P. Aji, T. Triyono, E. P. Budiana, and A. R. Prabowo, "Mechanical and Microstructural Properties of A36 Marine Steel," 2021.

[18] S. Shaikh, S. Shajib, A. Kader, D. Mondal, and A. Islam, "Effect of Preheating on Microstructure and Mechanical Properties in Mild Steel Arc Weld Joints," vol. 22, no. 1, pp. 12133–12145, 2025.

[19] D. S. Yasmin, F. Paundra, E. Pujiyulianto, F. T. Industri, I. T. Sumatera, and L. Selatan, "Effect of Welding Current on Low Carbon Steel CHARACTERISTICS IN SMAW," vol. 25, no. 1, pp. 1–7, 2025.

[20] J. He *et al.*, "Effect of Preheat Temperature and Welding Sequence on the Temperature Distribution and Residual Stress in the Weld Overlay Repair of Hydroturbine Runner," 2022.